The chemical and geometrical genesis of quasicrystals: relationship of icosahedral aluminum alloy quasicrystal structures to icosahedral structures in elemental boron

R. Bruce King
Department of Chemistry, University of Georgia, Athens, GA 30602 (U.S.A.)

(Received September 3, 1990)

Abstract

Chemically based structural models of icosahedral aluminum alloy quasicrystals use lattices of polyhedra of icosahedral local symmetry which are closely related to icosahedral structures found in boron chemistry, particularly the two rhombohedral allotropes of elemental boron. The structures of both β-rhombohedral boron and cubic R-Al_5CuLi_3 can be constructed from 60-vertex truncated icosahedra (the 'C_{60} polyhedron') but linked in very different ways in a three-dimensional crystalline lattice. Electron-precise models for the chemical bonding topology of both structures can be described using methods similar to those used to treat isolated globally delocalized deltahedral boranes such as $B_{12}H_{12}^{2-}$. In the structure of R-Al_5CuLi_3 the truncated icosahedra form the surfaces of 84-vertex Samson complexes retaining icosahedral local symmetry where each of the peripheral vertices is shared with an adjacent Samson complex leading to 54-atom building blocks. Simple pairwise rotation of the 30 pairs of vertices connecting pentagonal faces in the peripheral truncated icosahedron of each 54-atom building block in this lattice leads to a closely related lattice of 54-atom Mackay icosahedra. Such processes may convert crystal lattices such as R-Al_5CuLi_3 into closely related icosahedral quasicrystal structures such as T2-Al_5CuLi_3.

Introduction

One of the most exciting recent developments in materials science has been the discovery of aluminum alloys exhibiting diffraction patterns with apparently sharp spots containing five-fold symmetry axes [1, 2]. This discovery raises a crystallographic dilemma since the sharpness of the diffraction peaks suggests long-range translational order, as in periodic crystals, but five-fold axes are incompatible with such periodicity. Such materials are described as quasicrystals [3, 4], which are defined to have delta-functions in their Fourier transform but local point symmetries incompatible with periodic order. The structures of these materials may be viewed as three-dimensional analogues of Penrose tiling [5–8] which is a geometric structure exhibiting five-fold symmetries and Bragg diffraction. Location of atoms in quasicrystals requires the use of six-dimensional crystallography [9, 10] in which the atoms correspond to three-dimensional hypersurfaces in six-dimensional periodic lattices. For this reason the chemical structures of quasicrystals are not readily described in ways familiar to chemists. Chemically based models for quasicrystal structures are therefore more readily developed by first considering closely related true crystalline materials and then introducing appropriate perturbations destroying the periodic translational order but retaining the long-range translational and orientational order characteristic of quasicrystals [3, 4].

In considering the chemistry of icosahedral quasicrystals (i.e. those having five-fold symmetry) a striking observation is the presence of aluminum in almost all such materials [11, 12]. Aluminum is a congener of boron, which forms icosahedra in discrete molecular and ionic species such as $C_2B_{10}H_{12}$ [13] and $B_{12}H_{12}^{2-}$ [14] as well as infinite solid state materials such as boron-rich borides and several allotropes of elemental boron [15–17]. The proposed designation of the B, Al, Ga, In, Tl column of the Periodic Table as 'icosogens' [18] is also supported by the existence of Ga_{12} icosahedra in intermetallic phases such as $RbGa_7$, $CsGa_7$, Li_2Ga_7, K_3Ga_{13} and $Na_{22}Ga_{39}$ [18–20].

This paper examines the relationship of chemically based structural models of icosahedral aluminum alloy quasicrystals to the icosahedral structures found in boron chemistry, particularly the two rhombohedral

0020-1693/91/$3.50

allotropes of elemental boron. The phase Al_5CuLi_3 is selected as an example of an icosahedral aluminum alloy since appropriate structural models for this phase and closely related cubic phases have been developed by Audier and collaborators [21]. This paper thus considers the structural and electronic effects of increasing the packing density of icosahedral atomic aggregates in three-dimensional space starting with the discrete ion $B_{12}H_{12}^{2-}$ and then going successively to the simple (α) [22] and complicated (β) [23–25] forms of rhombohedral boron. Further increase in the packing density of icosahedral building blocks then leads to the Audier structure [21] for cubic R-Al_5CuLi_3. Simple atomic motions in this structure can then destroy the periodic translational order while retaining the long-range translational and orientational order required for quasicrystals.

Polyhedra of icosahedral symmetry

The icosahedral phases of interest have local icosahedral (I_h) symmetry and thus must have structures constructed from atoms at the vertices of polyhedra of icosahedral symmetry. Such polyhedra are depicted in Figs. 1 and 2, their properties are summarized in Table 1, and their symmetries are depicted in Fig. 3 [26]. The six polyhedra listed in Table 1 correspond to three pairs of dual polyhedra. In this context a given polyhedron P is converted to its dual P* by locating the vertices of P* above the midpoints of the faces of P and connecting two vertices of P* by an edge if and only if the corresponding faces of P share an edge [27]. A pair of dual polyhedra P and P* has the following properties:

(i) the numbers of vertices and edges in a pair of dual polyhedra satisfy the relationships $v=f^*$, $e=e^*$, $f=v^*$;

(ii) dual polyhedra have the same symmetry elements and thus belong to the same symmetry point group (I_h in the cases discussed in this paper);

(iii) the numbers of edges meeting at a vertex of P correspond to the numbers of edges in the corresponding face of P^*;

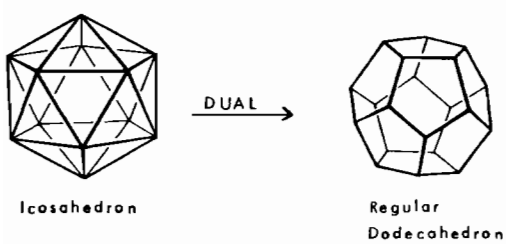

Fig. 1. The icosahedron and its dual, the regular dodecahedron.

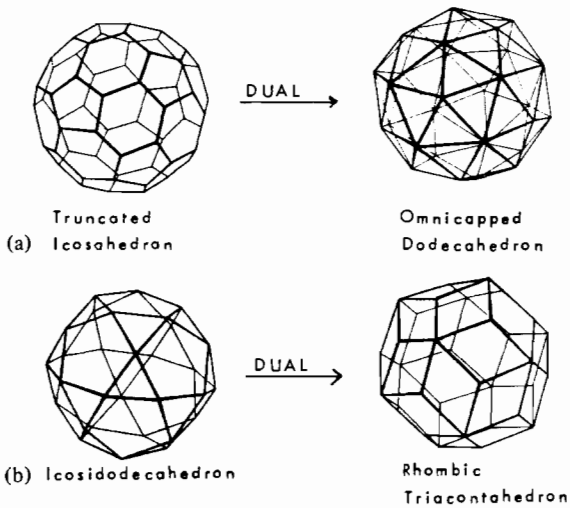

Fig. 2. (a) The truncated icosahedron ('C_{60} polyhedron') and its dual, the omnicapped dodecahedron; (b) the icosidodecahedron and its dual, the rhombic triacontahedron.

(iv) $(P^*)^* \approx P$, i.e. the dual of a dual of a polyhedron is topologically identical to the original polyhedron.

The three pairs of dual polyhedra of icosahedral symmetry depicted in Figs. 1 and 2 are the following.

(i) The regular polyhedra of icosahedral symmetry, namely the icosahedron itself and its dual, the regular (pentagonal) dodecahedron (Fig. 1).

(ii) The 60-vertex semiregular truncated icosahedron postulated [28] for the structure of C_{60} ('Buckminsterfullerene') and its dual, the 60-face omnicapped dodecahedron (Fig. 2(a)).

(iii) The 30-vertex icosidodecahedron and its dual, the 30-face rhombic triacontahedron (Fig. 2(b)). The 30 vertices of an icosidodecahedron are located at the 30 edge midpoints of an underlying icosahedron. The rhombic triacontahedron is an example of a zonohedron [7, 29], which is a polyhedron in which all faces are centrosymmetric and bounded by pairs of equal and parallel faces. Both of these polyhedra are relevant in understanding the structures of icosahedral quasicrystals.

Boron icosahedra

The prototypical example of an isolated boron icosahedron is found in the borane dianion $B_{12}H_{12}^{2-}$. In $B_{12}H_{12}^{2-}$ each boron atom provides the four valence orbitals of its sp^3 manifold. One of these four orbitals (an sp hybrid) is used for external bonding to a hydrogen atom whereas the remaining three orbitals are available as internal orbitals for the skeletal bonding of the boron icosahedron. Of the three internal orbitals on each boron atom, two equivalent orbitals (the twin internal or tangential

TABLE 1. Some polyhedra of icosahedral symmetry

Polyhedron	Vertices	Edges	Faces	Types of vertices[a]				Types of faces[b]				
				v_3	v_4	v_5	v_6	f_3	f_4	f_5	f_6	
Icosahedron	12	30	20	0	0	12	0	20	0	0	0	Dual pair
Regular dodecahedron	20	30	12	20	0	0	0	0	0	12	0	
Truncated icosahedron	60	90	32	60	0	0	0	0	0	12	0	Dual pair
Omnicapped dodecahedron	32	90	60	0	0	12	20	60	0	0	0	
Icosidodecahedron	30	60	32	0	30	0	0	20	0	12	0	Dual pair
Rhombic triacontahedron	32	60	30	20	0	12	0	0	30	0	0	

[a] v_n refers to the number of vertices having n edges meeting at that vertex (i.e. vertices of degree n). [b] f_3, f_4, f_5, and f_6 refer to the numbers of triangular, quadrilateral, pentagonal and hexagonal faces, respectively.

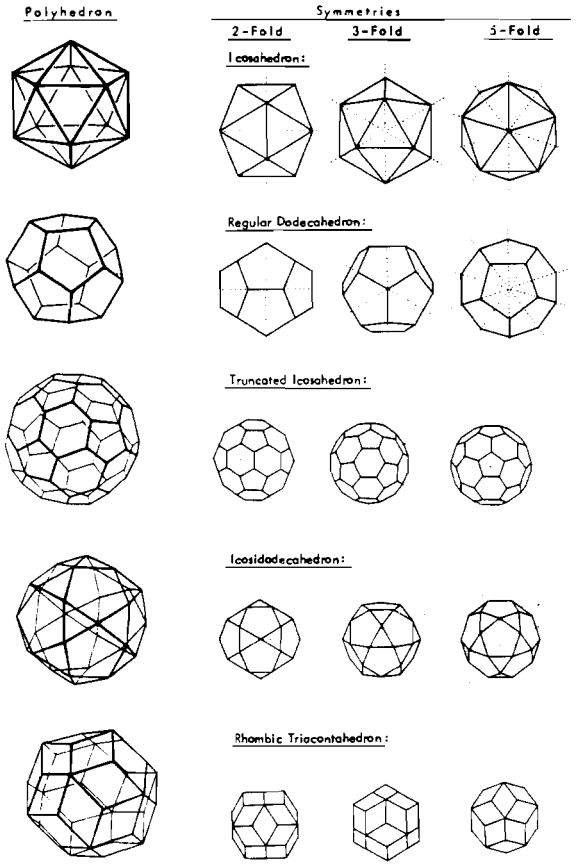

Fig. 3. The two-fold, three-fold and five-fold rotation axes in five polyhedra of icosahedral symmetry.

orbitals) are p orbitals which participate in bonding on the icosahedral surface. The remaining internal orbital (an sp hybrid) participates in a 12-orbital core bond in the center of the icosahedron leading to the global delocalization [30] of $B_{12}H_{12}^{2-}$. The $B_{12}H_{12}^{2-}$ anion has a total of (12)(3)+12+2=50 valence electrons of which 24 electrons are used in 12 two-center bonds to the external hydrogen atoms, 24 electrons are used for the skeletal surface bonding, and 2 electrons are used for the single 12-orbital skeletal core bond leading to a closed shell electronic configuration. A number of approaches [30–32] have been used to describe the bonding in deltahedral boranes such as $B_{12}H_{12}^{2-}$.

Elemental boron exists in a number of allotropic forms of which four (two rhombohedral forms and two tetragonal forms) are well established (Table 2). The structures of all of these allotropic forms of boron are based on various ways of joining B_{12} icosahedra using the external orbitals on each boron atom. The structures of the two rhombohedral forms of elemental boron are of interest in illustrating what can happen when icosahedra are packed into an infinite three-dimensional lattice. Note that in rhombohedral structures the local symmetry of an icosahedron is reduced from I_h to D_{3h} because of the loss of the five-fold rotation axes. The twelve vertices of an icosahedron, which are all equivalent under I_h local symmetry, are split under D_{3h} local symmetry into two non-equivalent sets of six vertices each (Fig. 4) [16]. The six rhombohedral vertices (circled vertices in Fig. 4) define the directions of the rhombohedral axes. The six equatorial vertices (uncircled vertices in Fig. 4) lie in a staggered belt around the equator of the icosahedron. The six rhombohedral and six equatorial vertices form prolate and flattened oblate trigonal antiprisms, respectively.

TABLE 2. Allotropic forms of elemental boron

Type	Structural units	Literature reference
α-Rhombohedral	B_{12}	22
β-Rhombohedral	$B_{12}(B_6)_{12}(B_{10})_2B$	24
α-Tetragonal	$(B_{12})_4(B)_2$	33
β-Tetragonal	$(B_{12})_8(B_{21})_4(B)_{10}$	34

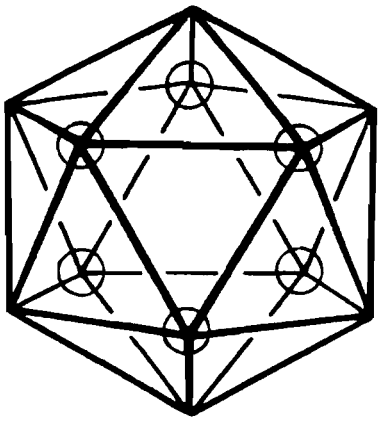

Fig. 4. The six rhombohedral vertices (circled vertices) and six equatorial vertices (uncircled vertices) of an icosahedron.

In the simple (α) rhombohedral allotrope of boron all boron atoms are part of discrete icosahedra. In a given B_{12} icosahedron the external orbitals of the rhombohedral borons are each used to form a two-center bond with a rhombohedral boron of an adjacent B_{12} icosahedron and the external orbitals of the equatorial borons are each used to form a three-center bond with equatorial borons of two adjacent B_{12} icosahedra. The available (12)(3) = 36 electrons from an individual B_{12} icosahedron are fully used as follows.

Skeletal bonding

12-center core bond:	2 electrons
12 2-center surface bonds: (12)(2) =	24 electrons

External bonding

(a) Rhombohedral borons:	
1/2 of 6 2-center bonds: (6/2) (2) =	6 electrons
(b) Equatorial borons:	
1/3 of 6 3-center bonds: (6/3) (2) =	4 electrons
Total electrons required:	36 electrons

α-Rhombohedral boron thus has a closed-shell electronic configuration.

The structure of the complicated (β) rhombohedral allotrope of boron avoids the three-center intericosahedral bonding of α-rhombohedral boron but is considerably more complicated. This structure is best described as a rhombohedral packing of B_{84} polyhedral networks known as Samson complexes (Fig. 5) [35] linked by B_{10} polyhedra and an interstitial boron atom so that the fundamental structural unit is $B_{84}(B_{10})_{6/3}B = B_{105}$. The idealized isolated B_{84} Samson complexes have I_h local symmetry which is distorted to D_{3h} in the rhombohedral local environment of the lattice. Within the B_{84} Samson complex the external orbital of each of the twelve boron atoms of a central B_{12} icosahedron forms a two-center bond with the external orbital of the apical boron of a

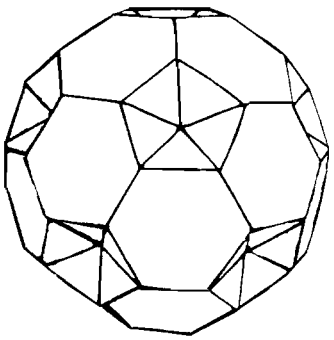

Fig. 5. A view of the surface of a Samson complex showing six of the twelve pentagonal pyramid cavities.

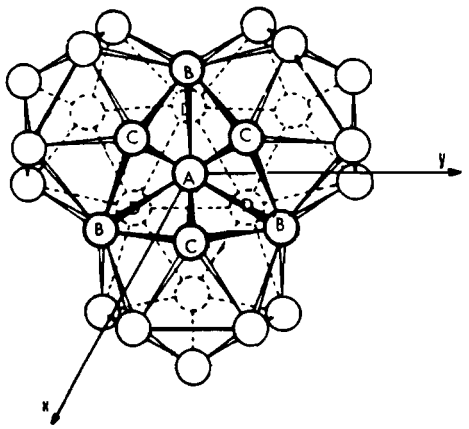

Fig. 6. The B_{28} polyhedron linking three Samson complexes in the β-rhombohedral boron structure.

B_6 pentagonal pyramid (i.e. a half-icosahedron) leading to the $B_{12}(B_6)_{12} = B_{84}$ stoichiometry. The external surface of this B_{84} Samson complex (Fig. 5) is a B_{60} truncated icosahedron (Fig. 2). The B_6 pentagonal pyramids in the rhombohedral positions (see Fig. 4) of the central B_{12} icosahedron of the B_{84} Samson complex overlap with analogous B_6 pentagonal pyramids of adjacent B_{84} Samson complexes to form six new B_{12} icosahedral cavities. The B_6 pentagonal pyramids in the equatorial positions (see Fig. 4) of the central B_{12} icosahedron of the B_{84} Samson complex each overlap with the corresponding equatorial B_6 pentagonal pyramids of two adjacent B_{84} Samson complexes by means of an additional B_{10} unit (vertices A, B, C and D in Fig. 6) to form new polyhedra of (3)(6) + 10 = 28 boron atoms (Fig. 6). These B_{28} polyhedra have local C_{3v} symmetry and are constructed by fusion of three icosahedra so that in each icosahedron one vertex (A in Fig. 6) is shared by all three icosahedra and four vertices (B and D in Fig. 6) are each shared by two of the icosahedra so that 3 $(B_7B_{4/2}B_{1/3}) = B_{28}$. Additional features of the structure of β-rhombohedral boron include the following:

(i) partial occupancy (73.4%) [25] of three of the boron vertices (D in Fig. 6) of the B_{10} unit linking three B_6 pentagonal pyramids to form the B_{28} polyhedron;

(ii) an interstitial boron atom (B(15) in the structural papers [25]) within bonding distance of six of the above partially occupied boron vertices corresponding approximately to an isolated tetracoordinate boron atom (i.e. $(0.734)(6) = 4.4$);

(iii) partial boron occupancy (24.8%) [25] of an interstitial site in the B_{84} Samson complexes (B(16) in ref. 25).

In order to consider an electron counting scheme for β-rhombohedral boron it is first necessary to consider the chemical bonding topology of the idealized B_{28} polyhedron (Fig. 6) formed by the fusion of three globally delocalized [30, 36, 37] boron icosahedra. The 28 boron atoms furnish a total of $(28)(4) = 112$ orbitals of which 24 orbitals (one on each boron atom except for boron atoms A and B in Fig. 6) are required for external bonding leaving $112 - 24 = 88$ atomic orbitals for the skeletal (internal) bonding. A 12-center core bond in each of the three icosahedral cavities of the B_{28} polyhedron requires $(3)(12) = 36$ atomic orbitals leaving $88 - 36 = 52$ atomic orbitals for pairwise surface bonding corresponding to 26 surface bonds. Thus a closed shell electronic configuration for the B_{28} polyhedron with one electron in each external orbital is B_{28}^{2+} requiring 82 electrons as follows.

24 external two-center bonds: $(24/2)(2) =$	24 electrons
3 12-center core bonds: $(3)(2) =$	6 electrons
26 surface bonds: $(26)(2) =$	52 electrons
Total electrons required:	82 electrons

The ~2/3 partial occupancy of three boron positions (D in Fig. 6) in the B_{28} polyhedron necessitated by the availability of only four valence orbitals of the interstitial boron (B(15) in ref. 25) for chemical bonding corresponds approximately to removing one of these borons from each B_{28} polyhedron. Removal of this boron atom to give a B_{27} polyhedron removes three electrons and four orbitals. Loss of these four orbitals has the following three effects:

(i) one external bond is eliminated reducing the required number of electrons by one;

(ii) one core bond is reduced from a 12-center bond to an 11-center bond with no effect on the required number of electrons;

(iii) one surface bond is eliminated reducing the required number of electrons by two. Thus the removal of one D vertex in the B_{28} polyhedron removes three electrons but also the need for three electrons ($3 = 1 + 0 + 2$ from (i), (ii) and (iii) above, respectively) so that the net charge on the species with the closed shell electronic configuration is not affected.

Next the roles of the two types of interstitial borons in β-rhombohedral boron must be considered. The boron atom in the fully occupied interstitial site (B(15) in ref. 25) bonded to four boron atoms of the B_{27} polyhedron (D in Fig. 6) has a closed shell configuration B^- (compare BH_4^- or $B(C_6H_5)_4^-$). The ~25% occupancy of the other six interstitial sites in each B_{84} Samson complex (B(16) in ref. 25) provides another $B_{1.5}$ to a fundamental structural unit. This additional $B_{1.5}$ provides an extra $(1.5)(3) = 4.5$ electrons without adding any new bonding orbitals since the atomic orbitals of these latter interstitial boron atoms merely increase some two-center surface bonds to three-center bonds.

All of these considerations indicate a fundamental $B_{104.5}$ structural unit for β-rhombohedral boron, which can be dissected as follows.

	Boron atoms	Net charge
Central B_{12} icosahedron	12	−2
6/2 Rhombohedrally located peripheral B_{12} icosahedra:		
$(6/2)(12) =$	36	
$(6/2)(-2) =$		−6
6/3 Equatorially located peripheral B_{27} polyhedra:		
$(6/3)(27) =$	54	
$(6/3)(+2) =$		+4
1 B(15) interstitial boron atom:	1	−1
$(0.25)(6) = 1.5$ B(16) interstitial boron atoms:		
$(1.5)(1) =$	1.5	
$(1.5)(+3) =$		+4.5
Total boron atoms and overall net charge	104.5	−0.5

The net charge of −0.5 for a 313.5 valence electron structural unit can be assumed to be zero within the experimental error of partial occupancies etc., indicating that β-rhombohedral boron, like the much simpler α-rhombohedral boron, has a closed shell electronic configuration. Note that in the lattices of both rhombohedral forms of boron the six rhombohedral and six equatorial borons of a central B_{12} icosahedron are linked to two and three other such B_{12} icosahedra, respectively, using simple two-center and three-center chemical bonds, respectively, for α-rhombohedral boron but using B_{12} icosahedra and B_{28} polyhedra (Fig. 6), respectively, for β-rhombohedral boron.

Icosahedral quasicrystals

There are several classes of icosahedral quasicrystals with diverse compositions [11]. The following classes are the most important:

(1) the i(Al–Mt) class (Mt = transition metal) including i($Al_{80}Mn_{20}$) [1], i($Al_{74}Mn_{20}Si_6$) [38, 39], i($Al_{79}Cr_{17}Ru_4$) [40];

(ii) the i(AlZnMg) class including i($Al_{25}Zn_{38}Mg_{37}$) [41], i($Al_{44}Zn_{15}Cu_5Mg_{36}$) [42] and i($Al_{60}Cu_{10}Li_{30}$) [43].

All of these phases contain relatively large amounts of aluminum suggesting the comparison of the structures of these materials with those of the icosahedral boron derivatives discussed above.

Consider the i($Al_{60}Cu_{10}Li_{30}$) system and related alloys containing aluminum, lithium, and copper and/or zinc, which have been studied in detail by Audier and collaborators [21]. This system is significant since there are crystalline phases of stoichiometries similar to the T2 icosahedral quasicrystal phases. The atom positions in the crystalline cubic R phase of approximate Al_5CuLi_3 stoichiometry are known so that the structure of this phase can provide some insight into the structure of the closely related T2 icosahedral phase of approximate stoichiometry [21] $Al_{0.570}Cu_{0.108}Li_{0.322}$. Of interest in the structure of R-Al_5CuLi_3 is the presence of discrete Al_{12} icosahedra indicating the icosogen nature of aluminum like its congeners boron and gallium [18].

Audier and collaborators [21, 44] have described a polyhedral shell structure for R-Al_5CuLi_3 using some of the polyhedra of icosahedral symmetry listed in Table 1 and depicted in Figs. 1 and 2 (see Fig. 6 in ref. 21 or Fig. 2 in ref. 44). This shell structure consists of the following layers:

(a) a central (Al, $Cu)_{12}$ icosahedron;

(b) an Li_{20} regular dodecahedron with the Li positions above the faces of the central (Al, $Cu)_{12}$ icosahedron (layer a) analogous to the construction of dual polyhedra discussed above;

(c) a larger (Al, $Cu)_{12}$ icosahedron formed from the external orbitals of the central (Al, $Cu)_{12}$ icosahedron (layer a) so that its atoms lie above the twelve faces of the Li_{20} dodecahedron in another 'polyhedral dual construction';

(d) An (Al, $Cu)_{60}$ truncated icosahedron (Figs. 2 and 7) distorted from I_h local symmetry to O_h symmetry so that 12 vertices are of one type (circled in Fig. 7) and 48 vertices are of another type (not circled in Fig. 7). The atoms of this polyhedron lie above the midpoints of the faces of the omnicapped dodecahedron (Fig. 2) formed by combining the Li_{20} dodecahedron (layer b) with the larger (Al, $Cu)_{12}$ icosahedron (layer c) in still another 'polyhedral dual construction', since the truncated icosahedron is the dual of the omnicapped dodecahedron (Fig. 2).

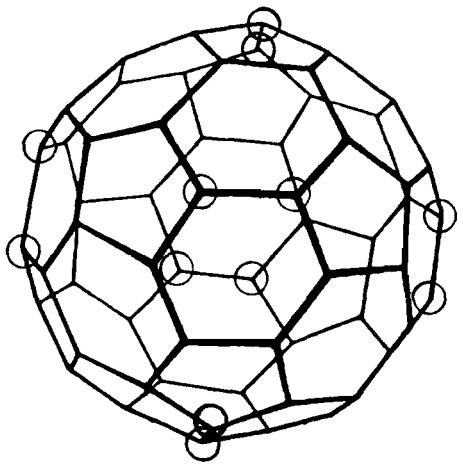

Fig. 7. The two different types of vertices in the (Al, $Cu)_{60}$ truncated icosahedron distorted from I_h to O_h symmetry found in the structure of cubic R-Al_5CuLi_3.

The (Al, Cu) subskeleton (layers a + c + d discussed above) in R-Al_5CuLi_3 forms a lattice containing 84-vertex Samson complexes (Fig. 5) identical to the B_{84} Samson complex in the β-rhombohedral boron lattice discussed above. However, the packing of the (Al, $Cu)_{84}$ Samson complexes in the R-Al_5CuLi_3 lattice is totally different from the packing of the B_{84} Samson complexes in β-rhombohedral boron. The (Al, Cu) subskeleton of the R-Al_5CuLi_3 lattice thus consists of a CsCl-type cubic packing of the (Al, $Cu)_{84}$ Samson complexes so that each atom of the peripheral (Al, $Cu)_{60}$ truncated icosahedron of the (Al, $Cu)_{84}$ Samson complex is shared with an adjacent Samson complex in one of the following two ways.

(i) The six edges connecting the six pairs of circled vertices in Fig. 7 lie in the faces of a cube and are shared with the corresponding edges of the adjacent Samson complex in the adjacent cube sharing the face containing the edge in question.

(ii) The eight hexagonal faces of the peripheral (Al, $Cu)_{60}$ truncated icosahedron *not* containing any circled vertices in Fig. 7 are shared with the corresponding faces of the adjacent Samson complex in the cube sharing the vertex lying at the end of the body diagonal of the original cube containing the midpoint of the hexagonal face in question.

The basic structural unit of the (Al, Cu) subskeleton of R-Al_5CuLi_3 thus is (Al, $Cu)_{54}$ = (Al, $Cu)_{12}$ + (Al, $Cu)_{12}$ + (Al, $Cu)_{60/2}$ corresponding, respectively, to the layers a + c + d discussed above. In addition to the 20 lithium atoms in layer b, additional lithium atoms (layer e) are located above the twelve pentagonal faces of the peripheral truncated icosahedra, which, because of the way the truncated icosahedra are linked, simultaneously cap the pentagonal faces

of two adjacent truncated icosahedra sharing an edge (sharing method (i) above). The sum of the number of atoms in layers a through e, respectively, in this model is $(Al, Cu)_{12} + Li_{20} + (Al, Cu)_{12} + (Al, Cu)_{60/2} + Li_{12/2} = (Al, Cu)_{54}Li_{26}$ corresponding to an (Al + Cu)/Li ratio of 2.08 in close agreement with 2.12 implied by the $Al_{0.564}Cu_{0.116}Li_{0.32}$ stoichiometry.

Now consider the electron counting in R-Al_5CuLi_3. In the (Al, Cu) subskeleton the aluminum and copper atoms function as donors of three and one electrons, respectively, assuming in the case of copper a stable d^{10} configuration corresponding to Cu^+. The lithium atom is a one-electron donor by ionization to Li^+. The stoichiometry $Al_{0.564}Cu_{0.116}Li_{0.32}$ coupled with the Audier model [21, 44] for R-Al_5CuLi_3 leads to the stoichiometry $Al_{45}Cu_9^{26-}$ for the fundamental Samson complex structural unit corresponding to (45)(3) + (9)(1) + 26 = 170 electrons. In addition application of the same Audier model to the cubic R phase of the Al–Cu–Li–Mg alloy of stoichiometry $Al_{0.52}Cu_{0.15}Li_{0.25}Mg_{0.08}$ leads to the stoichiometry $Al_{42}Cu_{12}Li_{20}Mg_6 = Al_{42}Cu_{12}^{32-}$ for its fundamental Samson complex structural unit also corresponding to (42)(3) + (12)(1) + 32 = 170 electrons. This suggests that 170 electrons is a 'magic number' for the 54-atom Samson complex structural unit of cubic crystalline aluminum alloy phases closely related to the icosahedral quasicrystals of the i(AlZnMg) class. This model assumes that the aluminum and copper atoms in these structures occupy the vertices of the Samson complexes (layers a, c, and d in the Audier model) and the more electropositive metals (Li and Mg) occupy interstitial positions (layers b and e in the Audier model).

The topology of the 84-atom Samson complex (Fig. 4) and the linkages of such complexes in a CsCl-type cubic lattice in R-Al_5CuLi_3 are consistent with the observed 170 electrons corresponding to a closed shell electronic configuration with delocalized bonding in polyhedral cavities of the following two types.

(i) The central $(Al, Cu)_{12}$ icosahedron (layer a) having the required (2)(12) + 2 = 26 skeletal electrons for globally delocalized chemical bonding topology similar to $B_{12}H_{12}^{2-}$.

(ii) The twelve pentagonal pyramid $(Al, Cu)^a(Al, Cu)^b_{5/2}$ cavities (layers c and d) where $(Al, Cu)^a$ refers to the single apical atom and $(Al, Cu)^b_{5/2}$ refers to the five basal atoms; each of the basal atoms is part of two different pentagonal pyramid cavities forming parts of different Samson complexes and thus has only two internal orbitals to contribute to the skeletal bonding of a given pentagonal pyramid cavity. In the view of the surface of the Samson complex in Fig. 5 six of the pentagonal pyramid cavities can be seen.

The *nido* bonding [30, 31, 32, 36, 45] in a pentagonal pyramid leading to $2n + 4 = 16$ skeletal electrons and eight bonding orbitals requires (6)(3) = 18 internal orbitals. However, in the pentagonal pyramid cavities in the Samson complex in the R-Al_5CuLi_3 structure there are only 3 + (5)(2) = 13 internal orbitals. For this reason only one five-center core bond and four two-center surface bonds are possible using these 13 internal orbitals leading to 10 rather than 16 skeletal electrons for each pentagonal pyramid. The chemical bonding topology for a $(Al, Cu)_{12}(Al, Cu)_{12}(Al, Cu)_{60/2}$ Samson complex outlined in Table 3 can lead to the observed 170 electrons while using the available 4 (12 + 12 + 60/2) = 216 valence orbitals of the sp^3 manifolds of the 54 vertex atoms.

The above discussion considers a model for the structure of the crystalline cubic R-Al_5CuLi_3. Now consider possible perturbations in this model to give the quasicrystal T2-Al_5CuLi_3. In this connection the 54-vertex Mackay icosahedron [46] (Fig. 8) appears as a structural unit in certain quasicrystals [9, 47].

TABLE 3. Electron and orbital counting in a Samson complex structural unit in R-Al_5CuLi_3

	Total electrons	Total orbitals
(A) 1 central $(Al, Cu)_{12}$ icosahedron (layer a)		
Core bonding: 2 electrons; 12 orbitals ×1 =	2	12
Surface bonding: (12)(2) = 24 electrons; 24 orbitals ×1 =	24	24
(B) 12 two-center bonds between the external orbitals of the central $(Al, Cu)_{12}$ icosahedron (layer a) and the $(Al, Cu)_{12}$ icosahedron in the next layer (layer b) (2 electrons; 2 orbitals) × 12	24	24
(C) 12 $(Al, Cu)^a(Al, Cu)^b_{5/2}$ pentagonal pyramid cavities (layer d)		
Core bonding (5-center): 2 electrons; 5 orbitals ×12 =	24	60
Surface bonding: (4)(2) = 8 electrons; 8 orbitals ×12 =	96	96
Total electrons and orbitals per $(Al, Cu)_{12}(Al, Cu)_{12}(Al, Cu)_{60/2}$ Samson complex	170	216

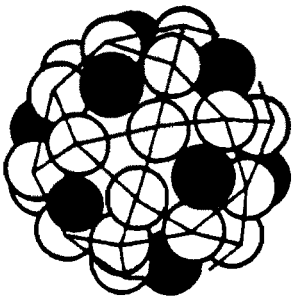

Fig. 8. A view of the surface of a Mackay icosahedron showing the vertices of the larger icosahedron (layer b) as black circles and the vertices of the icosidodecahedron (layer c) as white circles. The vertices of the central icosahedron (layer a) are not visible.

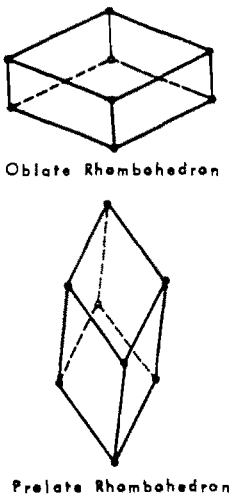

Fig. 9. The oblate and prolate rhombohedra used in a three-dimensional analogue of Penrose tiling to give a lattice of rhombic triacontahedra.

The Mackay icosahedron has a shell structure consisting of the following layers:

(a) a central icosahedron (not visible in Fig. 8);

(b) a larger icosahedron formed from the external orbitals of the atoms in the central icosahedron (layer a) overlapping with an additional set of twelve atoms (black circles in Fig. 8);

(c) a 30-vertex icosidodecahedron (Fig. 2) formed by placing atoms above each of the 30 edges of the larger icosahedron (layer b). Layer c is shown as white circles in Fig. 8.

Layers a and b of the Mackay icosahedron are identical to the first two layers of the Samson complex (i.e. layers a and c in the Audier model for R-Al_5CuLi_3) whereas the outer icosidodecahedron layer of the Mackay icosahedron (layer c) has exactly half the number of atoms of the outer truncated icosahedron in the Samson complex. Furthermore, the packing of the Samson complexes into the R-Al_5CuLi_3 lattice results in each of the peripheral truncated icosahedron atoms being shared between exactly two adjacent complexes (see above) so that a single Samson complex structural unit has the same 54 atoms as a corresponding Mackay icosahedron. This suggests a very close relationship between the packing of Samson complexes in the R-Al_5CuLi_3 crystal and a possible packing of Mackay icosahedra in a T2-Al_5CuLi_3 quasicrystal. In fact a concerted 90° rotation about a tangential axis of each of the 30 edges connecting pairs of pentagonal faces in the peripheral truncated icosahedron in each Samson complex of the R-Al_5CuLi_3 crystalline lattice converts a lattice of 54-atom Samson complexes into a lattice of 54-atom Mackay icosahedra. This type of process may be crucial in converting crystals built from icosahedral building blocks to quasicrystals and resembles 'martensitic' transformations such as those found in A-15 superconductors [48].

The final point of interest is the relationship of these models for quasicrystals to three-dimensional analogues of Penrose tiling [4–8, 49, 50]. Consider the Audier model [21, 46] for R-Al_5CuLi_3 discussed above. The center $(Al, Cu)_{12}$ icosahedron (layer a) and the Li_{20} regular dodecahedron (layer b) can be combined to form a 32-vertex rhombic triacontahedron (Fig. 2). Such rhombic triacontahedra resulting from capping the 20 faces of an icosahedron followed by deletion of the original 30 edges of the icosahedron can be constructed by an appropriate packing of ten oblate and ten prolate rhombohedra (Fig. 9) in a three-dimensional analogue of Penrose tiling discussed in detail elsewhere [4, 7, 8, 49, 50].

References

1 D. Shechtman, I. Blech, D. Gratias and J. W. Cahn, *Phys. Rev. Lett., 53* (1984) 1951.
2 D. Shechtman and I. A. Blech, *Metall. Trans., 16A* (1985) 1005.
3 D. Levine and P. J. Steinhardt, *Phys. Rev. Lett., 53* (1984) 2477.
4 D. Levine and P. J. Steinhardt, *Phys. Rev. B, 34* (1986) 596.
5 N. de Bruijn, *Ned. Akad. Weten. Proc. Ser. A, 43* (1981) 39.
6 N. de Bruijn, *Ned. Akad. Weten. Proc. Ser. A, 43* (1981) 53.
7 A. L. Mackay, *Sov. Phys. Crystallogr., 26* (1981) 517.
8 A. L. Mackay, *Phys. Status Solidi A, 114* (1982) 609.
9 V. Elser and C. L. Henley, *Phys. Rev. Lett., 55* (1985) 2883.
10 P. Bak, *Phys. Rev. Lett., 56* (1986) 861.
11 C. L. Henley, *Comments Cond. Mat. Phys., 13* (1987) 59.
12 C. Janot and J. M. Dubois, *J. Phys. F, 18* (1988) 2303.

13 R. N. Grimes, *Carboranes,* Academic Press, New York, 1970.
14 E. L. Muetterties (ed.), *Boron Hydride Chemistry,* Academic Press, New York, 1975.
15 W. N. Lipscomb and D. Britton, *J. Chem. Phys., 33* (1960) 275.
16 J. L. Hoard and R. E. Hughes, in E. L. Muetterties (ed.), *The Chemistry of Boron and its Compounds,* Wiley, New York, 1967, pp. 25–154.
17 D. Emin, T. Aselage, C. L. Beckel, I. A. Howard and C. Wood, (eds.), *Boron-Rich Solids,* American Institute of Physics Conf. Proc. 140, American Institute of Physics, New York, 1986.
18 R. B. King, *Inorg. Chem., 28* (1989) 2796.
19 C. Belin and R. G. Ring, *J. Solid State Chem., 48* (1983) 40.
20 J. K. Burdett and E. Canadell, *J. Am. Chem. Soc., 112* (1990) 7207.
21 M. Audier, C. Janot, M. de Boissieu and B. Dubost, *Philos. Mag. B60* (1989) 437.
22 B. F. Decker and J. S. Kasper, *Acta Crystallogr., 12* (1959) 503.
23 R. E. Hughes, C. H. L. Kennard, D. B. Sullenger, H. A. Weakliem, D. E. Sands and J. L. Hoard, *J. Am. Chem. Soc., 85* (1963) 361.
24 J. L. Hoard, D. B. Sullenger, C. H. L. Kennard and R. E. Hughes, *J. Solid State Chem., 1* (1970) 268.
25 B. Callmer, *Acta Crystallogr., Sect. B, 33* (1977) 1951.
26 P. Pearce and S. Pearce, *Polyhedra Primer,* Van Nostrand Reinhold, New York, 1978.
27 B. Grünbaum, *Convex Polytopes,* Interscience, New York, 1967, pp. 46–51.
28 H. W. Kroto, J. R. Heath, S. C. O'Brien, R. F. Curl and R. E. Smalley, *Nature (London), 318* (1985) 162.
29 H. S. M. Coxeter, *Regular Polytopes,* Pitman, New York, 1947, pp. 27–32.
30 R. B. King and D. H. Rouvray, *J. Am. Chem. Soc., 99* (1977) 7834.
31 D. M. P. Mingos, *Chem. Soc. Rev., 15* (1986) 31.
32 A. J. Stone and M. J. Alderton, *Inorg. Chem., 21* (1982) 2297.
33 J. L. Hoard, R. E. Hughes and D. E. Sands, *J. Am. Chem. Soc., 80* (1958) 4507.
34 M. Vlasse, R. Naslain, J. S. Kasper and K. Ploog, *J. Solid State Chem., 28* (1979) 289.
35 L. Pauling, *Phys. Rev. Lett., 58* (1987) 365.
36 R. B. King, in R. B. King (ed.), *Chemical Applications of Topology and Graph Theory,* Elsevier, Amsterdam, 1983, pp. 99–123.
37 R. B. King, *J. Math. Chem., 1* (1987) 249.
38 P. Guyot and M. Audier, *Philos. Mag., B52* (1985) L15.
39 L. A. Bendersky and M. J. Kaufman, *Philos. Mag., B53* (1986) L75.
40 P. A. Bancel and P. A. Heiney, *Phys. Rev. B, 33* (1986) 7917.
41 R. Ramachandrarao and G. V. S. Sastry, *Pramana, 25* (1985) L225.
42 N. K. Mukhopadhyay, G. N. Subbanna, S. Ranganathan and K. Chattopadhyay, *Scr. Metall., 20* (1986) 525.
43 P. Sainfort, B. Dubost and A. Dubus, *C. R. Acad. Sci. Paris, 301* (1985) 689.
44 M. Audier, J. Pannetier, M. Leblanc, C. Janot, J.-M. Lang and B. Dubost, *Phys. Status Solidi B, 153* (1988) 136.
45 R. Rudolph and W. R. Pretzer, *Inorg. Chem., 11* (1972) 1974.
46 A. L. Mackay, *Acta Crystallogr., 15* (1962) 916.
47 P. Guyot, M. Audier and R. Lequette, *J. Phys. (Paris), 47* (1986) C3.
48 R. Madar, J. P. Senateur and R. Fruchart, *J. Solid State Chem., 28* (1979) 59.
49 R. Penrose, *Bull. Inst. Math. Appl., 10* (1974) 266.
50 J. E. S. Socolar and P. J. Steinhardt, *Phys. Rev. B, 34* (1986) 617.